applied optics

X-ray reflective coatings made of Pt, Al_2O_3/Pt, and Al_2O_3/Ni/Pt produced by atomic layer deposition

David L. Windt,[1,*] Huazhi Li,[2] Dmitry Gorelikov,[2] Eric M. Gullikson,[3] Christian Gollwitzer,[4] Michael Krumrey,[4] and Christian Laubis[4]

[1]*Reflective X-ray Optics LLC, 425 Riverside Dr., Unit 16G, New York, New York 10025, USA*
[2]*Arradiance LLC, 11A Beaver Brook Road, Littleton, Massachusetts 01460, USA*
[3]*Lawrence Berkeley National Laboratory, 1 Cyclotron Road, Berkeley, California 94270, USA*
[4]*Physikalisch-Technische Bundesanstalt (PTB), Abbestraße 2-12, D-10587 Berlin, Germany*
**davidwindt@gmail.com*

Received 9 July 2024; revised 5 August 2024; accepted 5 August 2024; posted 6 August 2024; published 21 August 2024

The X-ray reflectance of Pt-based coatings deposited by atomic layer deposition (ALD) has been measured in support of assessing the feasibility of using this deposition method for the production of X-ray mirror coatings that can achieve high X-ray reflectance without causing unacceptably large degradation of mirror figure as a result of coating stress-driven substrate deformation. Specifically, reflectance measurements of single-layer Pt, Al_2O_3/Pt bilayer, and Al_2O_3/Ni/Pt trilayer coatings grown by ALD on flat Si substrates were made using synchrotron radiation at X-ray energies in the range from 0.35 to 10 keV, revealing that the reflectance of the bilayers and trilayers is superior to that of single-layer sputtered Ir below 3.5 keV. Single-layer Pt and Al_2O_3/Pt bilayer coatings produced using thermal ALD were also deposited onto both the front and back surfaces of thin, figured, sub-arcsecond-quality X-ray telescope mirror segments made of polished, single-crystal Si, without discernible degradation of surface figure. These results, along with the successful implementation of batch-coating of two such mirrors simultaneously with high-reflectance coatings grown by thermal ALD, demonstrate the viability of employing stress-balanced, double-sided ALD coatings to mitigate substrate deformation resulting from film stress in high-reflectance coatings. This approach may thus enable the mass production of high-performance, sub-arcsecond X-ray telescope mirrors.

https://doi.org/10.1364/AO.535173

1. INTRODUCTION

Mirrors used for the construction of grazing-incidence X-ray telescopes require optical coatings having high X-ray reflectance in order to maximize telescope collection efficiency. Further, the development of methods to mitigate mirror deformation due to film stress in such coatings is crucially needed to prevent degradation of angular resolution in the case of telescopes for future X-ray astronomy missions now being planned, such as Lynx [1] and others, that are envisioned to have higher angular resolution than those used for past missions, and that may be constructed from thin, precisely formed, segmented mirror substrates [2]. Single-layer coatings such as Ir and Pt can provide high reflectance at soft X-ray energies when used at graze angles below the corresponding critical angles for total external reflection [3]; however, these materials typically have high film stress when deposited by magnetron sputtering using deposition conditions that produce films having optimally high density and low roughness [4,5], the specific attributes needed for high X-ray reflectance. A variety of sputtered bilayer and trilayer coatings have been shown recently to have both higher soft X-ray reflectance and lower film stress than single-layer Ir [6]; yet, even the lower stresses achieved with these sputtered bilayer and trilayer coatings are incompatible with sub-arcsecond angular resolution, unless methods can be demonstrated to sufficiently mitigate stress-driven substrate deformation resulting from these films. The development of such methods is thus an active area of investigation at present [7] that remains a high priority for X-ray astronomy [8,9].

Atomic layer deposition (ALD) is a thin-film growth technique based on self-limiting sequential surface reactions [10] that can be used (in certain cases) to conformally coat all surfaces exposed in the ALD reaction chamber simultaneously. In particular, ALD holds the potential to simultaneously deposit X-ray reflective coatings onto both the front and back surfaces of thin segmented mirror substrates, such that the front- and back-side film stresses may cancel, thereby mitigating stress-driven substrate deformation [11]. Furthermore, the ALD process can be scaled to enable batch-coating of multiple substrates simultaneously, potentially reducing the cost, complexity, and time required to fabricate the many thousands of individual

X-ray mirror segments that would be required for the construction of a lightweight, highly nested X-ray telescope such as the Lynx X-ray Mirror Assembly [12], in spite of ALD's inherently low deposition rates. ALD also could be used to deposit X-ray reflective coatings onto full shell X-ray telescope mirrors [13], an alternative approach that is also being considered for future X-ray astronomy missions [14].

The number of materials that are suitable for use in X-ray reflective coatings and that can be deposited by ALD is presently small in comparison to sputtering, because each new candidate material for ALD requires the development of suitable binary reaction sequence chemistry that is tailored to that material [12]. Nevertheless, Pt and Ir coatings have already been successfully deposited using ALD, in particular onto embedded optical surfaces in high-aspect-ratio X-ray optical structures, including both micro-pore optics [15–17] and critical-angle transmission (CAT) gratings [18].

Described here is an investigation of the performance of three different X-ray reflective Pt-based coatings produced using ALD and of their suitability for use in the construction of high-angular-resolution X-ray telescopes. We have measured the grazing-incidence X-ray reflectance of single-layer Pt, Al_2O_3/Pt bilayer and $Al_2O_3/Ni/Pt$ trilayer coatings, all grown using ALD; reflectance was measured with synchrotron radiation at X-ray energies in the range from 0.35 to 10 keV. Each film was found to have high X-ray reflectance that is close to the modeled results, and comparable to or greater than that of sputtered Ir within certain energy bands below ~3.5 keV, as explained below. In work described in more detail previously [19], we have simultaneously coated both the front and back surfaces of thin, figured, segmented Wolter-I X-ray telescope mirror substrates of sub-arcsecond quality made of single-crystal silicon with either Pt or Al_2O_3/Pt films deposited by ALD, and have measured the figure before and after coating to assess the ability of the stress-balanced, double-sided coating method to preserve mirror figure. In that work, two mirrors were batch-coated with single-layer Pt, and two were coated with Al_2O_3/Pt bilayers. Interferometry measurements indicated no discernable degradation of surface figure after coating in all cases; furthermore, re-measurements show no subsequent change in figure after a period of 18 months, suggesting that this "stress balancing" method used to mitigate stress-driven substrate deformation, using ALD coatings, could be insensitive to any intrinsic changes in film stress that may occur over time. The following sections of this manuscript describe in detail the X-ray reflectance measurements of the three Pt-based ALD films specified above, along with a brief summary of the previous stress-balanced coating investigation, and concluding with a summary of findings and their implications for X-ray astronomy instrumentation.

2. METHODS

Films for X-ray reflectance measurements were deposited onto polished 100 mm diameter Si (100) wafer substrates using an Arradiance GEMStar ALD system: thermal ALD processes at a temperature of 250°C were used for the Pt [20] and Al_2O_3 layers [21]; Ni was grown by plasma-enhanced ALD (PEALD) at 150°C, using a process that is proprietary to Arradiance. Approximate ALD growth rates were 0.11 nm/cycle for Al_2O_3, 0.1 nm/cycle for Ni, and 0.12 nm/cycle for Pt, with monolayer-growth cycle durations of 20, 125, and 91 s, respectively; effective deposition rates were thus 5.5×10^{-3} nm/s for Al_2O_3, 8.0×10^{-4} nm/s for Ni, and 1.32×10^{-3} nm/s for Pt. The Pt layers were deposited onto 2 nm thick Al_2O_3 nucleation layers in all cases. The target layer thicknesses were determined from the simulation results, following X-ray reflective film design principles described previously [6].

Coating reflectance was measured as a function of energy at a fixed graze angle of $\theta = 0.9°$ using synchrotron radiation. This angle was selected to facilitate comparison with previous measurements of similar films deposited by sputtering [6]. Reflectance measurements for energies below 1.25 keV were conducted at the Advanced Light Source, Berkeley [ALS] using the Center for X-ray Optics' Reflectometry Beamline 6.3.2 [22]. The beamline is optimized for high spectral purity and low stray light over the spectral range 25–1250 eV. Reflectance measurements above 0.6 keV were conducted at two beamlines in the PTB laboratory at BESSY II, Berlin: the soft X-ray beamline [23] equipped with a plane grating monochromator was used for photon energies up to 1.8 keV, and the FCM beamline [24] with a four-crystal monochromator was used for energies in the range from 1.75 to 10 keV. Both beamlines are optimized for high spectral purity, with low stray light and very low higher-spectral-order contributions. At the FCM beamline, higher-order power contributions are below 10^{-3} in the entire range and below 10^{-5} above 3 keV; the spectral resolving power is between 4×10^3 and 1.2×10^4. Semiconductor photodiodes are used at both beamlines to measure the incident and the reflected radiation intensities. Each of the three coated wafers was cleaved into separate sections to facilitate measurements at the two synchrotron facilities. ALS measurements were conducted approximately 4 months after film deposition, while PTB measurements were conducted approximately 12 months after deposition.

3. RESULTS

The X-ray reflectance curves measured for each film are shown in red in Figs. 1A–1C, along with calculated reflectance curves shown as green dotted lines in each case. (For clarity, overlapping portions of the data derived from the measurements at separate beamlines were eliminated for the graphs shown in Fig. 1, although good agreement was found between the ALS and PTB data sets, suggesting no significant degradation in coating reflectance during the 8 months of time that elapsed between these measurements.) The calculated reflectance curves were computed using bulk densities and using the layer thicknesses, interface widths, and surface roughnesses indicated in Fig. 1, values that were determined using the differential evolution fitting algorithm available in IMD [25]. While the measured reflectance is high and in reasonably good agreement with the calculation in each case, small disparities are evident between the measured and calculated curves. These disparities may be due to deviations in the optical constants of the constituent materials, possibly resulting from the incorporation of impurities, from variations from the assumed bulk film densities, or from deviations from the nominal stoichiometry in the particular case of

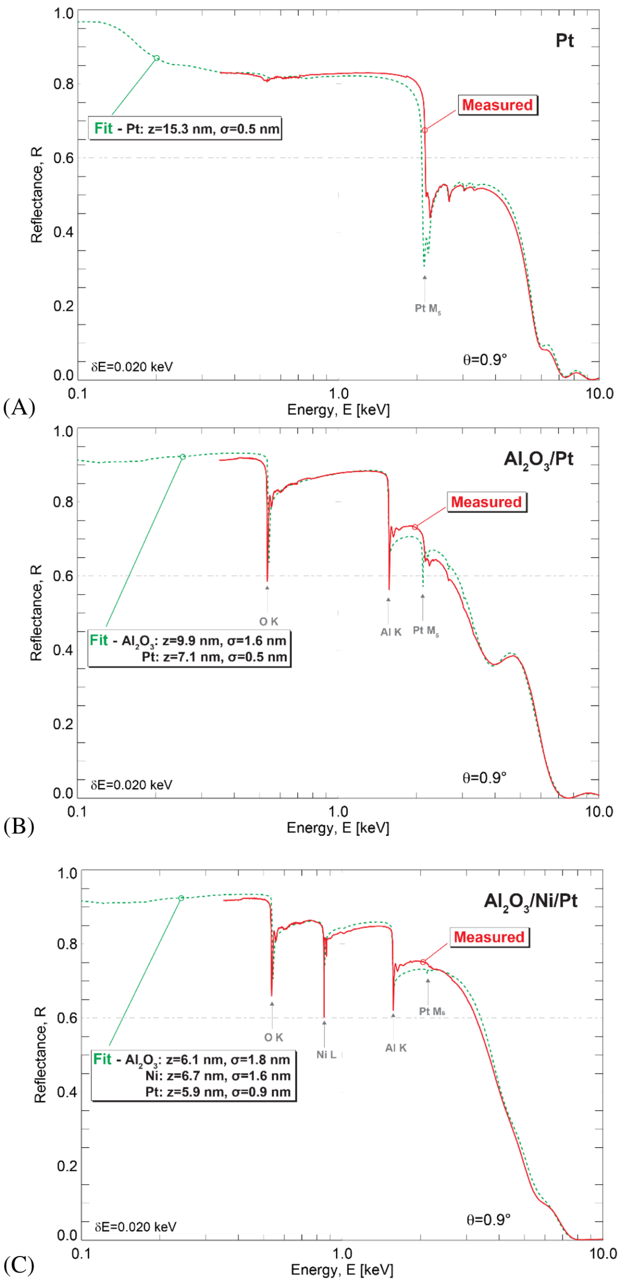

Fig. 1. Measured (solid red) and calculated (dotted green) X-ray reflectance as a function of energy at $\theta = 0.9°$ grazing incidence for (A) single-layer Pt, (B) Al_2O_3/Pt bilayer, and (C) Al_2O_3/Ni/Pt trilayer coatings deposited by atomic layer deposition. The best-fit layer thicknesses (z) and interface width/surface roughness values (σ) are indicated in the insets. The narrow drops in the reflectance are due to absorption that occurs near the binding energies of the K-, L-, and M-shell edges of the relevant materials in each case, as labeled.

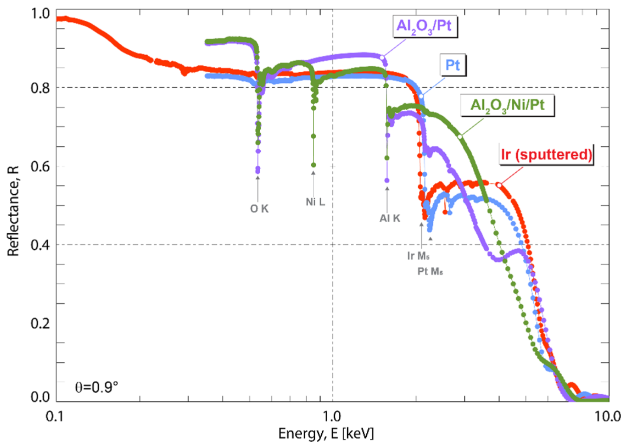

Fig. 2. Measured reflectance-versus-energy curves at $\theta = 0.9°$ for single-layer Pt (blue), Al_2O_3/Pt bilayer (violet), and Al_2O_3/Ni/Pt trilayer (green) coatings produced using ALD, in comparison with the measured reflectance of a sputtered Ir film (red) described previously.

the Al_2O_3 layers. The best-fit total film thicknesses are 15.3 nm for Pt, 17.0 nm for Al_2O_3/Pt, and 18.7 nm for Al_2O_3/Ni/Pt.

The measured reflectance curves of the three ALD films are shown together in Fig. 2, and in comparison with the measured reflectance of a sputtered Ir film (18.9 nm thickness) described previously [6]. The bilayer and trilayer ALD films provide higher reflectance than Ir in certain energy bands below ∼3.5 keV at this graze angle, excluding the narrow dips in reflectance due to increased absorption that occurs near the various elemental binding energies, which are labeled in Figs. 1 and 2. While the ALD Pt film provides reflectance that is comparable to the sputtered Ir film at energies below the Pt M-edge, the surface roughness of $\sigma = 0.3$ nm derived for the sputtered Ir film is substantially smaller than the $\sigma = 0.5$ nm surface roughness value derived for the ALD Pt film; larger surface roughness causes a larger reduction in specular reflectance relative to a perfectly smooth surface (i.e., for $\sigma = 0$), and an expected relative increase in non-specular (diffuse) scattering, although non-specular scattering was not measured for any films studied here.

As described in more detail previously [19], Pt-based ALD coatings were simultaneously deposited onto both the front and back surfaces of thin, figured, segmented Wolter-I X-ray telescope mirror substrates made of polished, single-crystal silicon; interferometric surface figure measurements were made before and after film deposition in order to quantify any change in figure due to the coatings. Four figured Si substrates were coated, two with single-layer Pt and two with Al_2O_3/Pt bilayer films, using the deposition conditions described above; the coatings are ostensibly identical to those shown in Figs. 1A and 1B, respectively. N.B.: The Al_2O_3/Ni/Pt coating shown in Fig. 1C was not used for this investigation due to the need to deposit Ni using PEALD, which is a direction-dependent process that could not be used to simultaneously coat all exposed mirror surfaces with sufficiently high uniformity. Two substrates were coated in each of two separate deposition runs, using the coating fixture shown in Fig. 3. Full-aperture cylindrical interferometry was used to measure the surface figure of the four substrates before and after coating; surface figure was also re-measured after a period of 18 months, during which time the substrates were stored in either dry nitrogen or in air. No discernable changes in surface height error were measured after coating, or after 18 months' storage, and no evident dependence on storage conditions was identified.

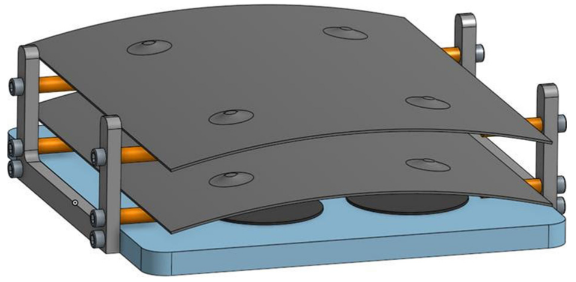

Fig. 3. Model of the fixture used to coat all exposed surfaces of two figured telescope mirror segments simultaneously by thermal atomic layer deposition.

4. SUMMARY AND DISCUSSION

Single-layer Pt, Al_2O_3/Pt bilayer and Al_2O_3/Ni/Pt trilayer coatings produced using ALD were all found to have high grazing-incidence X-ray reflectance in the energy band from 0.3 to 10 keV: the Pt coating was found to have reflectance that is close to that of a single-layer Ir film deposited by magnetron sputtering for energies below ∼2 keV, but reflectance that is approximately 10% lower than sputtered Ir at higher energies; the reflectance for both the bilayer and trilayer coatings was found to substantially exceed that of the Ir film in certain energy bands below ∼3.5 keV (at $\theta = 0.9°$), apart from narrow drops in reflectance due to absorption that occur near the K-, L-, and M-shell binding energies of the relevant materials (Figs. 1 and 2). Additionally, single-layer Pt and Al_2O_3/Pt bilayer coatings produced using thermal ALD were simultaneously deposited onto both the front and back surfaces of thin, figured, sub-arcsecond-quality X-ray telescope mirror segments made of polished, single-crystal Si, without discernable degradation of surface figure; re-measurements after 18 months of storage in either air or dry nitrogen indicate no subsequent changes in surface figure over time and no identifiable dependence on storage conditions. These experimental results, combined with the successful demonstration of batch-coating of two such mirrors simultaneously, illustrate the viability of using stress-balanced, double-sided thermal ALD coatings to mitigate stress-driven substrate deformation. Thermal ALD thus offers a feasible approach for the development of sub-arcsecond grazing-incidence X-ray telescopes constructed from thin, segmented telescope mirror substrates. Conformal coatings of Pt or Al_2O_3/Pt produced by thermal ALD could also be used with full shell X-ray telescope mirrors, in principle, as well as with high-aspect-ratio X-ray optical structures such as micro-pore optics and CAT gratings, in order to realize for those applications the performance benefits described above that these coatings can provide.

Funding. National Aeronautics and Space Administration (80NSSC18K0346).

Acknowledgment. The authors would like to thank Levent Cibik and Evelyn Handick for their contributions to the measurements at PTB, and William W. Zhang for his contributions to the surface figure investigations.

Disclosures. The authors declare no conflicts of interest.

Data availability. Data underlying the results presented in this paper are not publicly available at this time but may be obtained from the authors upon reasonable request.

REFERENCES

1. A. D. Falcone, R. P. Kraft, M. W. Bautz, *et al.*, "The high definition X-ray imager (HDXI) instrument on the Lynx x-ray surveyor," arXiv, (2018).
2. W. W. Zhang, M. P. Biskach, P. N. Blake, *et al.*, "High resolution and high throughput X-ray optics for future astronomical missions," Proc. SPIE **8861**, 8810N (2013).
3. D. Attwood, *Soft X-rays and Extreme Ultraviolet Radiation* (Cambridge University, 1999).
4. J. A. Thornton, "Influence of apparatus geometry and deposition conditions on the structure and topography of thick sputtered coatings," J. Vac. Sci. Technol. **11**, 666–670 (1974).
5. R. Messier, A. P. Giri, and R. A. Roy, "Revised structure zone model for thin film physical structure," J. Vac. Sci. Technol. A **2**, 312–315 (1984).
6. D. L. Windt, R. P. Conley, E. M. Gullikson, *et al.*, "Bilayer and trilayer X-ray mirror coatings containing W, Pt, or Ir in combination with C, C/Co, B_4C, or B_4C/Ni: x-ray reflectance, film stress, and temporal stability," Appl. Opt. **62**, 9568–9576 (2023).
7. P. M. Solly, W. W. Zhang, D. Windt, *et al.*, "Coating of thin, lightweight x-ray mirrors without distortion," Proc. SPIE **12181**, 121814P1 (2022).
8. "Astrophysics biennial technology report 2022," 20220002996, Astrophysics Division, Science Mission Directorate, NASA. 2022, https://ntrs.nasa.gov/citations/20220002996.
9. "2022 astrophysics strategic technology gaps," Astrophysics Division, Science Mission Directorate, NASA, https://apd440.gsfc.nasa.gov/tech_gap-descriptions.html.
10. S. M. George, A. W. Ott, and J. W. Klaus, "Surface chemistry for atomic layer growth," J. Phys. Chem. **100**, 13121 (1996).
11. K.-W. Chan, M. Sharpe, W. Zhang, *et al.*, "Coating thin mirror segments for lightweight x-ray optics," Proc. SPIE **8861**, 88610X (2013).
12. "Silicon meta-shell optics technology roadmap," NASA, 2019, https://wwwastro.msfc.nasa.gov/lynx/docs/documents/TechnologyRoadmaps/SMO_TR.pdf.
13. M. M. Civitani, G. Parodi, G. Vecchi, *et al.*, "Lynx x-ray optics based on thin monolithic shells: design and development," J. Astron. Telesc. Instrum. Syst. **5**, 021014 (2019).
14. "Full shell optics technology roadmap," NASA, 2019, https://wwwastro.msfc.nasa.gov/lynx/docs/documents/TechnologyRoadmaps/FSO_TR.pdf.
15. K. Takeuchi, Y. Ezoe, K. Ushikawa, *et al.*, "Pt thermal atomic layer deposition for silicon X-ray micropore optics," Appl. Opt. **57**, 3237–3243 (2018).
16. D. Ishi, Y. Ezoe, K. Ishikawa, *et al.*, "Enhanced X-ray reflectivity from Pt-coated silicon micropore optics prepared by plasma atomic layer deposition," Appl. Phys. Express **13**, 087001 (2020).
17. L. Li, C. Zhang, J. Wang, *et al.*, "Study on the optical properties of iridium-coated lobster eye X-ray micro-pore optics," Opt. Mater. **142**, 114120 (2023).
18. R. K. Heilmann, A. R. Bruccoleri, J. Kolodziejczak, *et al.*, "Critical-angle X-ray transmission grating spectrometer with extended bandpass and resolving power > 10,000," Proc. SPIE **9905**, 99051X (2016).
19. R. E. Riveros, M. P. Biskach, K. D. Allgood, *et al.*, "Fabrication of monocrystalline silicon X-ray mirrors," Proc. SPIE **11119**, 1111908 (2021).
20. J. Xie, X. Yang, B. Han, *et al.*, "Site-selective deposition of twinned platinum nanoparticles on TiSi2 nanonets by atomic layer deposition and their oxygen reduction activities," ACS Nano **7**, 6337–6345 (2013).
21. H. Li, M. Moore, N. Sullivan, *et al.*, "Low-temperature atomic layer deposition of platinum using (Methylcyclopentadienyl) trimethylplatinum and ozone," Arradiance, 2015, https://arradiance.com/papers/2015%20Arradiance,%20Low-Temperature%20Atomic%20Layer%20Deposition%20of%20Platinum,Li.pdf.

22. E. M. Gullikson, S. Mrowka, and B. B. Kaufmann, “Recent developments in EUV reflectometry at the advanced light source,” Proc. SPIE **4343**, 363–373 (2001).
23. F. Scholze, B. Beckhoff, G. Brandt, *et al.*, “High-accuracy EUV metrology of PTB using synchrotron radiation,” Proc. SPIE **4344**, 402–413 (2001).
24. M. Krumrey and G. Ulm, “High-accuracy detector calibration at the PTB four-crystal monochromator beamline,” Nucl. Instrum. Methods A **467**–468, 1175–1178 (2001).
25. D. L. Windt, “IMD - Software for modeling the optical properties of multilayer films,” Comput. Phys. **12**, 360–370 (1998).